CellPress

Feature Review

Taking Aim at Moving Targets in Computational Cell Migration

Paola Masuzzo,[1,2] Marleen Van Troys,[2] Christophe Ampe,[2] and Lennart Martens[1,2,*]

Cell migration is central to the development and maintenance of multicellular organisms. Fundamental understanding of cell migration can, for example, direct novel therapeutic strategies to control invasive tumor cells. However, the study of cell migration yields an overabundance of experimental data that require demanding processing and analysis for results extraction. Computational methods and tools have therefore become essential in the quantification and modeling of cell migration data. We review computational approaches for the key tasks in the quantification of *in vitro* cell migration: image pre-processing, motion estimation and feature extraction. Moreover, we summarize the current state-of-the-art for *in silico* modeling of cell migration. Finally, we provide a list of available software tools for cell migration to assist researchers in choosing the most appropriate solution for their needs.

Trends

Cell migration is central to many physiological and pathological phenomena.

The field of cell migration is becoming a high-content, high-throughput discipline, with heterogeneous and rich datasets being continuously produced with different imaging modalities.

Computational methods and tools are therefore essential for the analysis of image-based cell migration experiments.

Iteration between *in silico* modeling and experimental procedures can enormously advance the knowledge of cell migration mechanisms.

We review common computational algorithms and software packages for the quantification and modeling of cell migration data.

Computational Cell Migration in a Nutshell

Cell migration plays a fundamental role in physiological phenomena including neural development, wound healing, and immune function, as well as in disorders such as neurological diseases, fibrosis, and cancer metastasis [1–8]. Investigation of cell migration is therefore essential for successful intervention in physiological and pathological phenomena [9–12]. A major driver in the advance of cell migration research has been the evolution of instrumentation (microscopes and cameras) and the corresponding development of experimental tools and biological models. Indeed, 2D *in vitro* assays [13,14] have recently given way to more sophisticated two-and-a-half-dimensional (2.5D) and 3D approaches [15,16] which more faithfully represent the tissue environment. Because *in vivo* experiments are difficult and costly, *in vitro* and *ex vivo* setups are widely used, especially in drug compound and gene screening [17,18]. This review therefore primarily focuses on the quantification of cell migration in *in vitro* setups, while we refer the reader to specific literature on *in vivo* work [19–23].

Instrumentation has been crucial in advancing cell migration research, especially the advent of high-throughput and high-content imaging systems. Indeed, live cell phase-contrast/fluorescence microscopy provides a powerful tool to generate quantifiable data, but this approach relies on image-processing algorithms to extract cell motion and morphology descriptors. Because of the complexity and amount of data obtained from such imaging-based experiments, an unmet need for bioinformatics solutions for data annotation, management, and sharing has emerged [24]. Moreover, the role of computational approaches also extends to mathematical modeling and *in silico* experiments [25]. Indeed, a pioneering study has shown the integration of *in vitro* setups with *in silico* modeling to be extremely powerful, especially for the characterization of cancer invasion and metastasis [26].

[1]Medical Biotechnology Center, VIB, Ghent, Belgium
[2]Department of Biochemistry, Ghent University, Ghent, Belgium

*Correspondence:
lennart.martens@vib-ugent.be
(L. Martens).

 http://dx.doi.org/10.1016/j.tcb.2015.09.003

While further advances in the field hinge on the use of computational tools and mathematical modeling, the application of these techniques typically requires a standard of knowledge in mathematics, physics, and computer science that often remains absent in cell biology research groups. Therefore, this review aims to help cell migration researchers decide upon a computational strategy for the analysis of their experiments by summarizing the available methods and tools for computational image processing and *in silico* modeling of cell migration.

Computational Image Processing of Cell Migration

A typical cell migration study combines live-cell microscopy with image-processing algorithms [27] (Figure 1A). After samples are prepared, usually in multiwell plates, automated image acquisition is carried out with a digital camera microscope equipped with a motorized *xyz*-stage and an acclimatization chamber. A variety of imaging techniques can be used in such a setup, and we refer to [28,29] for an overview. Because cell migration is a dynamic process that comprises temporal and spatial information, time-lapse microscopy experiments are typically conducted with moving cells imaged over several hours. Image processing then summarizes the acquired image sequences into numerical features. Downstream data analysis subsequently yields a final interpretation of the experiment.

The processing of a digital image is a multi-step operation (Figure 1B) which begins with low-level pre-processing, followed by motion estimation and feature extraction. Most of these steps are dependent on acquisition settings such as field of view, sampling time, and especially imaging modality.

Image Pre-Processing: Restoration

Before image processing, image quality issues must first be addressed to improve the signal-to-noise ratio (SNR). Different pre-processing steps are required for optical phase-contrast and

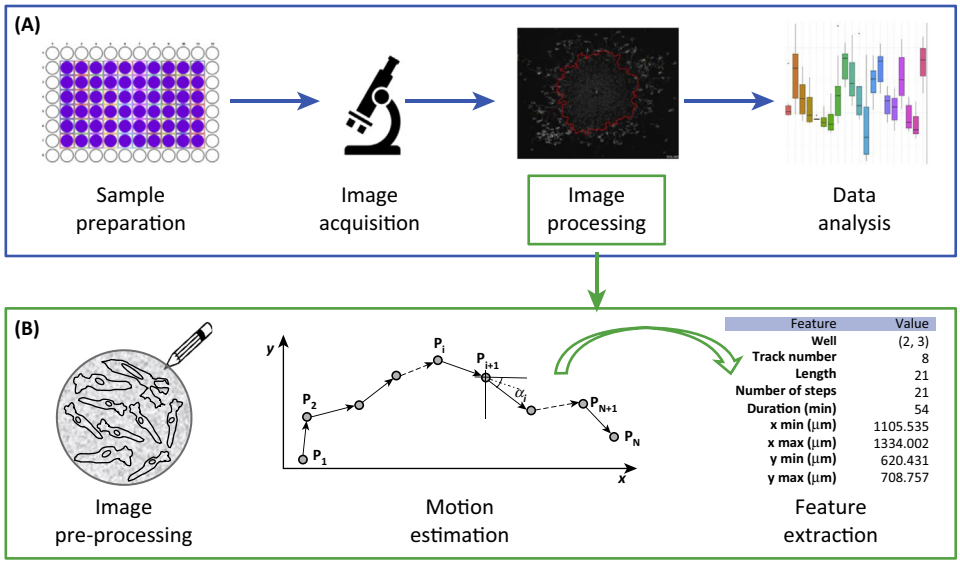

Figure 1. A Typical Workflow for an Imaging-Based Cell Migration Experiment. (A) After sample preparation, automatically acquired microscopy images are processed for subsequent data analysis and interpretation. (B) A common image-processing pipeline starts with the application of algorithms for image pre-processing; motion estimation is then achieved by applying computational image-processing algorithms; final feature extraction enables data analysis and interpretation of the cell migration experiment.

Glossary

Collective cell migration: coordinated movement of groups of cells that remain connected via cell–cell junctions. 2D sheet migration across a tissue surface, or multicellular strands or groups moving through a 3D tissue scaffold, represent forms of collective cell migration.

Diffusivity: the ability of a substance to undergo a diffusion process. In the case of cell migration, diffusion measurements are related to the mean squared displacement of a particle undergoing a Brownian motion.

Graphical user interface: software that works at the interface between a computer and its user, and employs graphic elements to simplify the use of a computer program.

Haar-like features: digital image features used in object recognition. These features consider adjacent regions in a detection window, and use the differences in global pixel intensities across these regions to categorize subsections of an image.

Linear discriminant analysis: a technique that finds a linear combination of features that characterize or separate two or more classes of objects. It is often used for dimensionality reduction before a classification task.

Machine Learning: a subfield of computer science that provides computers with the ability to learn without being explicitly programmed. Its goal is to devise algorithms that can learn from and make predictions about data.

Posterior density function: the density function describing the posterior probability of an event, in other words the probability that an event will occur after taking into consideration new information.

Principal component analysis: a technique that converts a set of observations of possibly correlated variables into a smaller set of values of linearly uncorrelated variables termed principal components.

Single-cell migration: a process that enables cells to move as single entities. Based on cell type, cytoskeletal structure, and protease production, this migration can occur in different morphological variants, such as mesenchymal and amoeboid.

fluorescence images. Phase-contrast images usually suffer from contrast and illumination problems, and therefore require image background detection, background filtering or masking, and histogram equalization. By contrast, fluorescence microscopy suffers from more intricate noise sources [30]. Indeed, non-desired signals can be generated by different structures (autofluorescent substrates or unspecific labeling) and can be subtracted by estimation of the average background. Median or anisotropic filtering can suppress noise coming from short exposure time or low excitation intensity. Moreover, deconvolution techniques have been developed to remove fluorescence from out-of-focus planes [31–33], thus enhancing image sharpness. Among the classical linear-deconvolution algorithms, the Wiener filter [34], and the Tikhonov–Miller filter [35] are widely used. The drawback of these linear filters is that they cannot restrict the solution domain with additional constraints, such as finite support, smoothness, regularization terms, or non-negativity. Non-linear deconvolution approaches can instead be used to incorporate such constraints [36] through iterative minimization of the error functions defined between the acquired image and the blurred estimate of the original object [37]. Examples of these constrained iterative deconvolution approaches include the Jansson–van Cittert [38] method and the classical maximum likelihood estimator [39]. These non-linear algorithms require more computational resources because of their iterative formulations; therefore, alternative, faster deconvolution techniques have been proposed based on wavelets [40], sparse representations [41], and space-variant blur approximations [42].

Tumor microenvironment: the cellular environment in which a tumor exists, including fibroblasts, immune cells, and cells that comprise the blood vessels.

Velocity correlation length: the length at which the spatial velocity correlation function decreases. Typically, this quantity is lower for cells whose migration is less collective.

Motion Estimation: Tracking

Cell tracking is performed on restored images to enable quantitative motion estimation. This requires *ad hoc* procedures that depend on the motility mode under investigation. Indeed, while some cells migrate individually in a **single-cell migration** (see Glossary) mode, cells can also retain cell–cell contacts and move as a single multicellular unit [43] in a **collective cell migration** mode [44,45].

Cell tracking has historically been performed manually, and this is still used today, for example, for benchmarking. For single-cell migration, an operator clicks on a reference point within a cell for each time-lapse frame. For collective cell migration, the operator must instead localize the edges of either a cell-free zone or a cluster of cells, again for each time-lapse frame. This manual technique is not only time-consuming but also imprecise and prone to user bias. Indeed, it is difficult to define a reference for cell positions, and considerable inconsistency occurs between different operators. This can also lead to a miscalculation of migration rates of up to 410% [46]. Automated cell tracking systems that can provide objective and robust migration rates are therefore highly desired. While manual tracking is still used to establish ground truth reference data for the evaluation and validation of novel algorithms [47,48], the large variability inherent in manual annotation casts some doubt on the reliability of such manually procured reference sets.

In the following paragraphs we present the most common automated cell tracking algorithms, according to the broad classification of 'tracking by detection', 'tracking by model evolution', and 'tracking by filtering' methodologies for 2D data, although this classification can also be used for 3D data (Box 1). We also discuss methods that address lineage events that confound cell tracking.

Tracking by Detection

In detection-based approaches, cells must first be separated from the background and from each other in a process termed segmentation. Segmentation divides an image into different segments that belong either to the objects of interest (groups of cells or single cells) or to the background. More precisely, image segmentation assigns a label to each pixel of an image such that pixels with the same label share particular characteristics. The simplest way to do this is to use a gray level threshold that labels pixels above an intensity cut-off as 'object' and the

Box 1. 3D Cell Migration

Studies of 3D cell migration have revealed several differences in cell behavior compared to analysis of 2D cell migration [15]. In the past 20 years, research strategies have therefore increasingly shifted towards 3D time-lapse (3D+t or, sometimes referred to as 4D in literature) imaging of migrating cells, both *in vitro* and *in vivo*. The analysis of complex 3D microscopy datasets brings many specific computational challenges in key processing tasks such as image registration, cell segmentation, and cell tracking. A major issue is the increased computational cost of the corresponding algorithms. In addition, the resolution of most confocal microscopy techniques in the *xy*-plane is at least threefold better than in the *z*-axis, requiring special adjustments to be made, such as image interpolation or anisotropic filtering. In 3D image processing, segmentation can be directly performed at each *xy*-plane, and then extended to the third dimension. However, this requires further computations to connect the 2D regions-of-interest along the *z*-axis. Given these computational challenges, few methods currently exist for automated 3D cell tracking, of which most have been developed to work with fluorescent microscopy. For example, a 2D particle-based tracking algorithm has been extended to 3D taking into account adjacent optical planes, thus inferring the cell motion along the *z*-axis [155]. One recent approach automatically detects and tracks many cells by using a kernel density estimation to convert each 3D image into a continuous function [156], while another uses a probabilistic graphic model [157]. Currently-available solutions for unlabeled cell tracking implement template-matching-based methods to deal with large populations of cells [158] or with fast-moving cells *in vivo* [159].

remainder as 'background' [49]. Disconnected segments of pixels can then be automatically classified as cells. However, a single threshold for a whole image is suboptimal in non-uniformly illuminated samples, where the SNR varies across the image. In these cases, it is better to use local adaptive thresholding, where each pixel receives a different threshold based on the intensity information in the local region. A comprehensive survey of methods to find optimal local thresholds is presented in [50].

Another common segmentation method is based on edge detection. This method relies on the principle that an edge or boundary in an image is related to a large change in image intensity [51]. While edge-detection methods are more robust than thresholding methods, they still fail on low-contrast images.

A limitation of both thresholding and edge-detection methods is their inability to distinguish between two objects of the same intensity that share a boundary, for example, when cells overlap or are adjacent. This limitation is overcome by the popular watershed method that considers the image as a topographic relief in which the gray level of a pixel is interpreted as its altitude. 'Flooding' this relief from the local intensity minima subdivides the image into regions and contours. Because this approach can lead to over-segmentation, specific pre- and post-processing techniques are typically used as well [52–54]. It is worth noting that many of the segmentation algorithms currently available rely on *a priori* knowledge of the typical diameter of the cells to be detected.

For collective cell migration, the segmentation task becomes a pure global background/foreground classification problem in which no explicit cell segmentation is performed. A cell boundary algorithm has been developed that can handle noise, local minima, and adjacent cells [55]. A custom multistep texture-segmentation algorithm has been proposed for bright-field wound-healing assays [56], while Bayesian classifiers have been shown to work well across diverse cell morphologies and imaging modalities [57]. **Machine Learning** has also been applied to this problem, employing a cascade of support vector machines to iteratively train and test classifiers centered on texture-based features [58].

The first benchmarks for multicellular segmentation algorithms have also been published recently [47]. Two freely-available tools (TScratch [59] and MultiCellSeg [58]) and one purpose-built algorithm [60] were evaluated on 171 segmented images of five cell lines from different laboratories, imaged under different conditions and at different confluence levels. The results show that algorithms tend to triumph when applied to the type of data they were designed for.

For instance, MultiCellSeg [58] prevails on differential interference contrast (DIC) images of DA3 cells in single-well experiments, while another algorithm [60] works best on DIC images of MDCK cells grown in microfluidic plates. Additional benchmarks can aid informed algorithm selection, and may boost more robust algorithm development as well.

Once cell positions have been identified, they need to be connected over time to form cell trajectories. The easiest way to accomplish this association task is to connect every segmented cell in a frame to the nearest cell in the subsequent frame. Here, 'nearest' may refer to the spatial location, and cell centroids can thus be used as reference points. This option works well if the cells are moving slowly with respect to the chosen frame-rate and are not densely packed. In other cases, a different approach termed feature matching gives better results. This method locates similar cells using an extended list of features such as morphology, volume, surface, and total curvature that expand the concept of distance beyond spatial location. Typically, these techniques require the user to specify the maximal distance that cells can travel between two consecutive timeframes. Furthermore, feature matching algorithms rely on good segmentation to keep the match as accurate as possible. Moreover, if a cell changes morphology between subsequent timeframes, it can be seen as two different cells, yielding broken trajectories.

Tracking by Model Evolution

This type of tracking uses a deformable model to describe each tracked object, and segmentation and tracking are performed simultaneously by fitting this model to the image data. The result of one frame is then used as an initial condition for the analysis of the next frame. This is usually done by evolving the contours of the cells in time [61]. Deformable models are given different names (snakes, active contours or surfaces, and balloons [62]) and come in two types: parametric [63] and geometric [64]. Parametric models are defined explicitly as parametric contours and are mostly used for 2D applications. These models allow fast, real-time implementations, but do not consider topological events such as track splitting or merging. By contrast, geometric deformable models (also known as level-set methods) [65–67] represent curves and surfaces implicitly as a level set of a higher-dimensional scalar function, thus capturing topological changes more easily. However, these methods require reinitialization in the case of fast motion with respect to the chosen frame-rate, or when cells appear or disappear from the field of view. Despite the intrinsic difference between parametric and geometric deformable models, they share an underlying principle: starting from a rough segmentation, the models are iteratively evolved to minimize a specific energy function.

The mean-shift algorithm, generalized in [68], also belongs to the tracking by model evolution category. It is an iterative procedure that seeks a local mode by shifting each datapoint to the average of the datapoints in its neighborhood, and thus does not rely on precise border detection. It works well for phase-contrast images where cells are often surrounded by bright halos, and can present membrane extensions out of the focal plane.

Tracking by Filtering

Particle-filtering techniques (also known as sequential Monte Carlo techniques [69]) are widely used in multiple-object tracking systems. Object tracking can be characterized as the problem of estimating the state of a system given a set of observations. The main idea behind particle-filtering methods is therefore to estimate an object's state **posterior density function** by a set of random particles with associated weights (Monte Carlo approximation, Figure 2). More specifically, the algorithm has three major steps, namely selection, prediction, and measurement, which are performed iteratively. After an initialization phase, the selection step generates a new particle set by choosing the particles with the highest posterior probability among the previous particle set. In the prediction step, each particle is modified according to the state model of the surrounding region-of-interest, while in a subsequent measurement step the weight

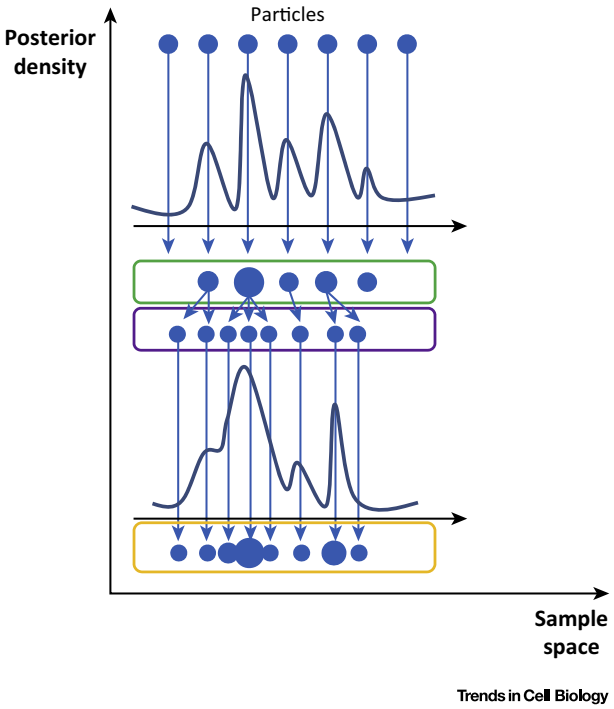

Figure 2. Schematic Representation of a Particle-Filtering Technique. In the selection step (in green) particles with the highest posterior probability are chosen; the prediction step (in purple) modifies each particle according to the state model; finally, in the measurement step (in orange), the weight of each particle is reevaluated based on the new data.

of each particle is reassigned based on the new data. To avoid the accumulation of weight by good particles and increased penalization of bad particles, a resampling step is often necessary. Finally, summing the weighted particles gives an approximation of the target distribution, and the most recent state estimation is then used to initialize the tracking of the next frame.

Many of the proposed particle filters for cell tracking in video sequences rely on a single feature. However, multiple-feature tracking provides a better description of the objects, and therefore improves the robustness of the method [70]. In most current particle-filtering methods, human interaction or another type of initialization is necessary to define the prior distributions of object states in the first frame. Furthermore, the deformation of the tracked object must remain small, which precludes their application to individual cell tracking where larger deformations are the norm.

Lineage Events

Lineage events such as mitosis, cell fusion, and apoptosis can confound tracking and can lead to incorrect object associations. Several methods have therefore been developed to detect these events. The most common approach to detect mitosis is based on the fact that such a cell path must have a Y-shape. Moreover, a mitotic cell displays a characteristic spatiotemporal pattern: it contracts, becomes rounder, and appears brighter in phase-contrast [71,72]. Probabilistic models exist as well, both for the identification of paths that contain a mitotic event and for the localization of a birth event [73] in phase-contrast microscopy. **Haar-like** elliptical **features**, with the addition of orientation, illumination, scale information, and edge and shape information, have recently allowed the detection of cell division events for 3D microscopy datasets as well [74].

Feature Extraction: Collective Cell Migration

Collective cell migration is essential in many biological processes, and is the most common motility pattern for many living organisms [4,5,44,75–77]. Among the *in vitro* cellular assays

normally used to probe collective cell migration, 2D wound-healing [78] and 2D/3D cell exclusion zone assays [18,79] are the most popular. In both types of assay, an artificial cell-free zone is created either by scratching a cell monolayer (see green area in Figure 3A1) or by using a plastic or Teflon separation device. Microfluidic devices [80] can be used in some applications, although their increased complexity reduces analysis throughput. We here consider the classic wound-healing assay to summarize quantitative features for collective cell migration because of its simplicity and its widespread use (Figure 3A1).

Quantification of collective cell migration is usually achieved using two measures: wound size and migration rate. Wound size is extracted by iterative image segmentation of the wound margins for

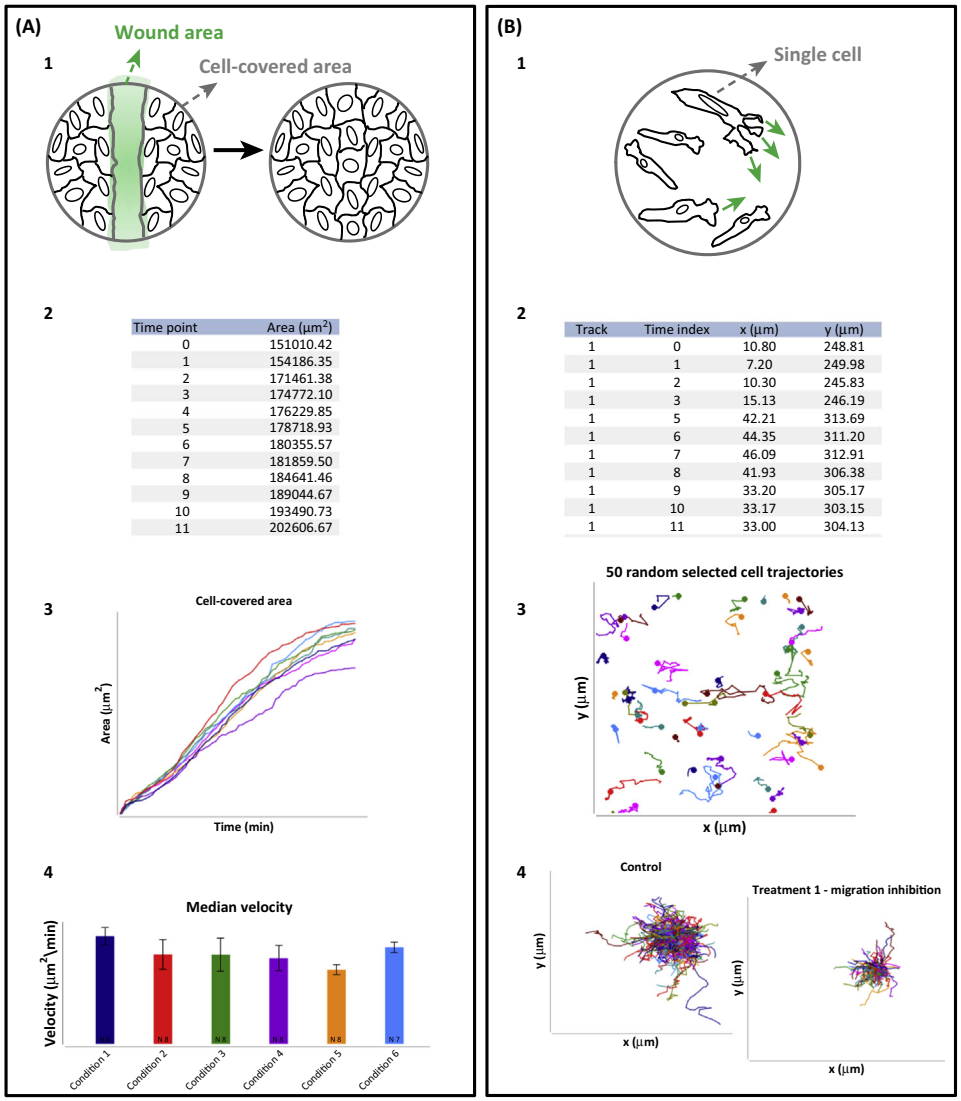

Figure 3. Quantification of a Cell Migration Experiment. (A) Collective cell migration: in a common wound-healing assay, a cell-free zone is created (wound area, in green), and the area evolution in time of either this zone or of the cell-covered zone is recorded (A2 and A3). The rate of change of this area is then computed, and used as a metric to extract velocity and/or compare different cell populations (A4). (B) Single-cell migration: *xy* positions are recorded in time (B2), and trajectories are reconstructed from these coordinates (B3). Single-cell tracks are then usually superimposed at the origin, allowing quick visual comparison of different cell populations (B4).

each time-lapse microscopy sequence. Software tools either quantify the wound area or the cell-covered area (Figure 3A2,A3). The migration rate can then be computed from: (i) differences in wound size over time [81], (ii) differences in wound size relative to the control [82], (iii) the percentage difference in the wound area [83], or (iv) the wound size at specific timepoints [84]. The rate of change of the wound area can be extracted using a linear regression model, and can be used for comparisons across different cell populations and treatments (Figure 3A4). The temporal evolution of the wound area can also be fitted to a Richards function (non-symmetrical sigmoid function), and the migration rate estimated as the maximum slope of the fitted curves, as in [60].

Whereas the tracking of only a few cells at the leading edge can be performed manually (as in [85]), accurate segmentation and automated tracking of all cells within a confluent sheet is a challenging computational task. Particle or cell image velocimetry (PIV/CIV) [86,87] is therefore often used as an alternative. These approaches map the velocity field within the cell monolayer via local correlations between successive images. In this way, measures such as the **velocity correlation length** are used to quantify the cellular coordination in the cell sheet, or in a specific part of the sheet, for example, in a finger-like extension at the wound edge [88,89].

Feature Extraction: Single Cell Migration

Single cell migration allows cells either to cover local distances and integrate into tissues, such as neural crest cell migration, or to move from one location in the body to another and fulfill effector functions, such as immune cell trafficking [90,91]. When cells migrate individually (Figure 3B1) the motion estimation is focused on their coordinates and the subsequent reconstruction of cell trajectories from those coordinates (Figure 3B2,B3). Usually, a simple linear interpolation is sufficient for track reconstruction if the image acquisition frame-rate takes into account the average migration speed of the studied cells. However, high-order interpolation schemes are sometimes necessary to achieve more accurate track representations. The cell trajectories are commonly visualized in a Rose plot, where coordinates are shifted to the origin of the space (i.e., normalized to the initial starting position for each detected cell), allowing cell trajectories across different experimental conditions to be inspected and compared (Figure 3B4). If the migration behavior is random, then the cell tracks will move out in all directions from the plot origin. Similarly, a preferred direction of movement will also be easily identified.

Given the cell trajectories, a long list of more informative measures can be derived [27,92,93] (Box 2). Step-centric variables are computed for an instantaneous translocation of a cell between two successive timeframes, while cell-centric variables describe the cell track in its total length, and are a direct result of summing or averaging step-centric data across all timeframes. Immediate step-centric measures are instantaneous displacement and turning angle. Other measures are connected with the rate of displacement, such as instantaneous speed. Cell-centric data include the cumulative and the net distance traveled in time by the cell and the end-point directionality ratio, also known as the confinement ratio, persistence ratio, meandering index, or straightness index. In addition to these displacement-related features, directionality-related features such as the average turning angle can also be computed. Commonly, the ratio of displacement to trajectory length is used to measure directional persistence. However, this measurement is biased, particularly by cell speed, and an unbiased alternative is to calculate direction autocorrelation as a function of time [94]. Another useful measure is the arrest coefficient, defined as the fraction of time that a cell is pausing. This last feature, however, relies on the choice of a minimum speed or translocation value for the definition of a cell in pause. Useful information can also be obtained from the convex hull for a cell track, that is, the smallest set of points that contains the track (Box 2). From this convex hull, outreach ratio, displacement ratio, and acircularity can be computed.

Box 2. Single-Cell Migration Features

When cells are tracked as individually moving objects, their spatial coordinates are recorded in time. Given a resulting cell trajectory, a full list of more informative measures can be derived. Figure I shows a 2D-recorded cell track consisting of N points $p_i = (x_i, y_i)$ (this 2D example can easily be extended to the 3D case; the inset in red represents the convex hull of this cell trajectory). Assuming a constant frame rate with a time interval Δt, and computing the distance (p_i, p_{i+1}) between two consecutive points with the Euclidean norm, the features presented in the Table can be derived.

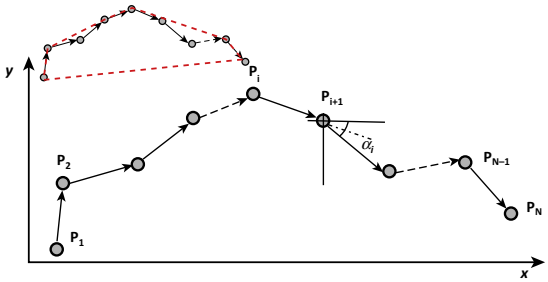

Single-cell migration features

Step-centric features	
Instantaneous displacement	$d_i = \sqrt{(x_{i+1} - x_i)^2 + (y_{i+1} - y_i)^2}$
Turning angle	$\alpha_i = \tan^{-1}[(y_{i+1} - y_i)/(x_{i+1} - x_i)]$
Direction autocorrelation	$dir\text{–}aut_i = \cos(\alpha_{i+1} - \alpha_i)$
Instantaneous speed	$v_i = d(\boldsymbol{p_i}, \boldsymbol{p}_{i+1})/\Delta t$
Cell-centric features	
Total distance traveled	$d_{tot} = \sum_{i=1}^{N-1} d(\boldsymbol{p_i}, \boldsymbol{p}_{i+1})$
Net distance traveled	$d_{net} = d(\boldsymbol{p_i}, \boldsymbol{p}_N)$
Mean curvilinear speed	$\bar{v} = (1/N-1)\sum_{i=1}^{N-1} v_i$
Mean straight-line speed	$v_{lin} = d_{net}/d_{tot}$
Directionality ratio	$dir = d_{net}/d_{tot}$
Convex hull	Smallest convex set containing all $\boldsymbol{p}_i$
Max distance traveled	$d_{max} = max_i\, d(\boldsymbol{p}_1, \boldsymbol{p}_i)$
Displacement ratio	$dr = d_{net}/d_{max}$
Outreach ratio	$dr = d_{max}/d_{tot}$
Convex hull perimeter	P
Convex hull area	A
Acircularity	$a = P^2/4\pi A$
Mean squared displacement	$MSD = (1/N-n)\sum_{i=1}^{N-n} d^2(\boldsymbol{p}_i, \boldsymbol{p}_{i+n})$

Trends in Cell Biology

Figure I. A Schematic Representation of a 2D Recorded Cell Track, Together with its Convex Hull, and a Table that Reports Single-Cell Migration Features.

Diffusivity variables can also be extracted, such as the mean squared displacement (MSD). The MSD–time curve indicates if the migration mode is freely diffusing, transported, or bound and limited. However, the underlying mechanism of migration cannot be entirely extrapolated from the MSD–time curve because different processes can lead to identical or highly similar MSDs. For example, similar MSD plots are obtained if T cell migration is considered either as consisting

of randomly oriented steps of fixed duration and speed, or as persistent movements with highly variable speed [95].

Feature Extraction: Cell Morphology

During cell tracking, software tools delineate cell shapes in each timeframe to derive position estimates, for example, from the cell centroids. The abovementioned features can then be computed from these positions. Measuring the cell shape in each frame, however, also allows the computation of cell morphology descriptors that can be used to describe cell size and orientation, or cell geometry. Cell size and orientation are determined through perimeter/surface and area/volume for 2D and 3D data, respectively, together with the lengths of the major and the minor axes. Cell geometry is computed by comparing the cell to the ellipse with the same second-moments as the original object region. Metrics representing geometrical complexity include eccentricity (the ratio between the foci of the ellipse and its major axis length), solidity (the ratio between the cell area and the convex hull area), extent (the ratio between the cell area and the bounding box area), and circularity (also called form factor, computed as $4\pi A/P^2$, where A and P are the area and the perimeter of the cell, respectively). For 2D data, more sophisticated analyses of cell morphology require the decomposition of the cell shape in Fourier terms or Zernike polynomials, while **principal component analysis** and **linear discriminant analysis** can be applied to data of any dimensionality. We refer to [96] for a thorough discussion on the computational analysis of cell shape.

Software Tools for Cell Migration Image Processing

A large variety of software tools are available for processing microscopy images of cells but, despite the recent advances of the field, not all of these implement algorithms for cell migration analysis. Most of the available software packages are developed for tracking fluorescently labeled cells, which is usually easier to achieve and requires less parameter tuning. Indeed, many of the computational techniques that are developed strongly rely on a set of conditions, such as image quality or predefined parameters, and will therefore only function properly if used on data obtained under similar conditions. This lack of robustness might explain why commercial software is usually restricted to labeled cell tracking, which is relatively robust after applying some standard contrast-enhancement techniques. For phase-contrast cell migration experiments, however, the field is still lacking robust software tools, especially when cells invade across 3D matrices. While there is no single criterion to decide which software package is most appropriate for the quantification of a specific cell migration experiment, Table 1 provides some guidance. Note that this table is not exhaustive because *ad hoc* software packages developed for specific cell migration-driven phenomena are not included. This is for instance the case for tools such as StarryNite [97], which is specifically designed for the study of embryogenesis.

Both free software solutions for general purpose (such as ImageJ/Fiji [98,99], CellProfiler [100], and ICY [101]), as well as commercial software packages (such as Volocity, ImarisTrack, and MetaMorph), offer diverse functions both for image pre-processing, segmentation, and cell tracking. ImageJ/Fiji, CellProfiler, and ICY greatly benefit from an extensible plugin architecture which allows developers to introduce new computational algorithms. Moreover, such plugins can expand the list of features that can be computed, thus allowing the creation of highly powerful and customized workflows. Conversely, the unique advantage of commercial software packages is their close integration with the instruments, which provides the ability to display the tracked results together with the original data. This allows easy verification of the tracking results and the possibility to present the data in a manner that outside observers can quickly understand.

Most of the tools reported in Table 1 are capable of tracking multiple cells at the same time, and allow the user to compute measures from the resulting cell trajectories. Other tools are

Table 1. An Alphabetical List of Commercial and Free Software Packages for Image Processing in Cell Migration Studies

Tool	Source	Platform/ Automation[a]	Application[b]	Output Format	Computed Features
Commercial Tools					
CELLMIA	DciLabs/ UGent[1]	Windows/A	2D/3D PC, FL	Tab-delimited text	Number of cells, number of tracks, cell positions, cell displacements, cell turning angle, directionality metrics, cell area (for bulk cell populations)
Cell motility BioApplications	Thermo Scientific[2]	Cross-platform/A	2D/3D FL	CellInsight CX5 HCS platform	Single cell and collective tracking
Image-Pro Plus	Media Cybernetics[3]	Windows/A	2D/3D PC, FL	MSExcel	Cell morphology, cell displacements, cell angles
ImarisTrack	BitPlane AG[4]	Windows, Mac/A	2D/3D PC, FL	MSExcel, comma-separated values	Number of cells, cell centroid positions, cell surface areas (2D), cell volumes (3D), cell displacements, cell velocities, path curvature, number of fusions of tracks, number of divisions of cell track
MetaMorph	Molecular Devices[5]	Windows/A	2D/3D PC, FL	MSExcel	Cell displacements, cell angles, cell velocities
OpenLab	PerkinElmer[6]	Mac/A	2D/3D FL	MSExcel, comma-separated values	Wound-healing measurements, percentage of wound closure
Free Tools					
Adapt	[160][7]	ImageJ; cross-platform/A	2D FL	Comma-separated values	Morphological features, velocity maps, cell trajectories
AveMap	[102][8]	MATLAB; Windows, Mac/A	2D PC	Tab-delimited text	Wound-healing measurements: local velocities, monolayer edges, wound area, wound shape, productive velocities
Cell Image Velocimetry	[89][9]	MATLAB; Windows/A	2D PC, FL	MATLAB mat	Wound-healing measurements, velocity fields, angular velocity distributions
CellCognition	[109][10]	Cross-platform/A	2D PC, FL	CellH5	Cell positions, cell shapes, convex hull features, intensity-based features, cell trajectories

Table 1. (continued)

Tool	Source	Platform/ Automation[a]	Application[b]	Output Format	Computed Features
CellProfiler	[100][11]	Cross-platform/A	2D FL	MSExcel	Cell displacements, cell velocities, cell morphology, area, perimeter, solidity, form factor, eccentricity
CellTrack	[106][12]	Windows; compiling from source required for other platforms/A	2D PC, FL	Tab-delimited text	Number of cells, boundary positions, cell speeds, path length, cell area, cell deformation
CellTracker	[161][13]	MATLAB; Windows/S	2D, FL	MSExcel, XML	Number of cells, cell centroid positions, cell surface areas (cytoplasm and nucleus individually), cell displacements, cell velocities
iTrack4U	[162][14]	Cross-platform/A	2D PC, FL	MSExcel, XML	Single cell tracking, speed, acceleration, angle, persistence, statistics on computed features
LineageTracker	[163][15]	Cross-platform/S	2D, FL	MSExcel	Nucleus areas, cell shapes, cell sizes, cell lineages
ManualTracking	[101][16]	ICY; cross-platform/M	2D/3D PC, FL	XML	Cell centroid positions
MtrackJ	[164][17]	ImageJ/Fij; cross-platform/M	2D/3D PC, FL	ImageJ data table	Cell centroid positions, cell displacements, cell velocities, cell angular changes
MultiCellSeg	[58][18]	MATLAB; Mac/A	2D PC	MATLAB mat	Wound-healing measurements: multicellular segmentation features
Pathfinder	[104][19]	Cross-platform/A	2D FL	MSExcel	Position, speed, direction, persistence
SpotTracking	[165][20]	ICY; cross-platform/A	2D/3D FL	XML	Cell displacements, cell velocities, trajectories editing
TScratch	[59][21]	MATLAB; Windows, Mac/A	2D PC	MSExcel	Wound-healing measurements: open wound area
TrackMate	[166][22]	ImageJ/Fij: cross-platform/A	2D/3D FL	ImageJ data table, XML	Cell displacements, cell velocities, cell orientations, trajectory length, trajectory displacement (enables manual editing of tracks)

Table 1. (continued)

Tool	Source	Platform/ Automation[a]	Application[b]	Output Format	Computed Features
u-track	[166][23]	MATLAB; Windows/A	2D FL	MATLAB structure array	Cell tracks merging, cell tracks splitting, cell displacements
Volocity Quantitation	PerkinElmer[24]	Windows, Mac/A	2D/3D FL	Tab-delimited text	Number of cells, cell centroid positions, cell surface areas (2D), cell volumes (3D), cell displacements, cell velocities

[a]Automation: A, automated; M, manual; S, semi.
[b]Application: PC, phase-contrast; FL, fluorescence.

specifically designed for the analysis of collective cell migration, such as the MATLAB toolbox Cell Image Velocimetry [89], and the stand-alone TScratch [59]. Classification of motility phenotypes by means of velocity maps is also possible for collective migration experiments with the AveMap tool [102], which makes use of the particle image velocimetry technique [86,87]. A community-driven initiative to develop free and open-source software for PIV analysis and post-processing has been recently launched in the form of the OpenPIV [103] framework which provides implementations in MATLAB, C++, and Python (www.openpiv.net). This initiative is promising, but, because it is still under development, it currently lacks good documentation, more advanced algorithms, and a user-friendly **graphical user interface**.

Some packages are able to bring single-cell and collective cell migration quantifications together. The algorithms implemented in the commercial package CELLMIA are capable of simultaneously tracking individual cells and delineating the cell-covered area of cells migrating as a sheet. The open-source Pathfinder [104] addresses individual migration of fluorescent cells, as well as their collective migration (here defined as cells migrating in the same direction). Tools that allow tracking of individual cells are usually equipped with options to export the tracking results to files, which can then be imported into downstream visualization and statistical software for final interpretation. Some other tools instead allow the tracking process to be viewed and/or edited through graphical user interfaces. This is, for example, the case for the Fiji plugin TrackMate [99].

The Open Source Computer Vision Library (OpenCV) [105] is an image-processing library on which customized solutions have been built for cell segmentation and tracking, for example, in the extensible and cross-platform package CellTrack [106]. Furthermore, the free scikit-image Python library [107] has recently been released, equipped with a rich list of image-processing algorithms. Moreover, the scikit-tracker package (http://scikit-tracker.org, still in an early stage of development) enables detection and tracking of cells, and interfaces with OME XML and OME TIFF [108], as well as with ImageJ [98], to handle file input and output. Finally, the CellCognition [109] framework was built for fluorescence time-lapse microscopy, allowing machine learning classification of cell morphologies with time-resolved analysis by single-cell tracking. It has a stand-alone application, the CecogAnalyzer, which enables object detection, feature extraction, tracking of individual cells over time, and detection of class-transition motifs, and stores the output in CellH5 [110] files.

In Silico Modeling of Cell Migration

Mathematical modeling and numerical simulations currently complement traditional experimental research in many scientific domains. Although 'real' experiments will always be needed to

advance our understanding of biological processes, *in silico* experiments can guide the wet-lab process by narrowing the experimental search space and potentially reducing experimental costs. Because modeling and simulation rely on experimental results to predict cell behavior that can then be tested experimentally, these methods integrate easily into the experimental cycle of cell biology [111–113].

The key advantage of *in silico* computational models is their ability to handle multiple interacting variables at the same time, and to alter these simultaneously, which is difficult to achieve in an experiment. Furthermore, models and computational predictions can also describe the behavior of the system as a function of only a single variable, a scenario often unattainable with current experimental techniques. In addition, mathematical models can identify key parameters that play a central role in defining the overall behavior of the system, and can thus suggest the most informative perturbations for follow-up experiments, even leading to novel *in vitro* approaches [26].

The combination of laboratory experiments with *in silico* modeling has been shown to be extremely powerful for cell migration research as well [114,115], especially for tumor invasion studies [26,116,117]. This importance derives from the inherent multiscale, multiparametric nature of cell migration: cell migration not only operates across multiple scales [118] (Table 2) but also requires multiple interlocked parameters [e.g., extracellular matrix (ECM) architecture and cellular determinants] to be combined in an integrated way, affecting the resulting migration mode [90]. Indeed, a recent study combined computational models and experiments to investigate the forces involved in adhesion-independent migration, showing that actin cortex flows drive cell movement through nonspecific substrate friction [119]. Furthermore, a generic model that explains migration transitions and that predicts a phase diagram of migration phenotypes based on confinement, adhesion, and contractility has been developed through a combination of mathematical modeling and experimental procedures [120].

A cell is a complex biological system with numerous components interacting across different organizational levels. To become the object of modeling and numerical simulation, a cell and its

Table 2. Investigating Cell Migration on Different Length-Scales

Scale	Computational method	Measurements	Challenges
Amino acid ($\leq 10^{-10}$ m)	Monte Carlo simulations, molecular dynamics	Effect of point mutation for migration-related diseases, e.g., cancer invasion	Difficult to connect with higher order scales and experiments High computational costs
Molecular (10^{-9} m)	Monte Carlo simulations, molecular dynamics, protein structure modeling, force-based dynamics Models	Signaling, protein structure, protein–protein interaction, protein–DNA interactions, and protein translocation	High computational costs
Macromolecular (10^{-9}–10^{-6} m)	Monte Carlo simulations, molecular dynamics, agent-based models	Focal adhesion formation, cell signaling, structure of protein complexes	Loss of molecular-scale detail
Single cell (10^{-6}–10^{-5} m)	Monte Carlo simulations, finite element models, agent-based models, reaction/diffusion models	Single-cell migration, adhesion, proliferation, signaling	Loss of spatial resolution at subcellular level Difficult to integrate biochemical and biomechanical events
Multicellular ($>10^{-5}$ m)	Continuous (deterministic) models, finite element models	Shape and structure of tissue, cell population response to forces and stimuli	Difficult to connect with molecular scale Difficult to integrate biochemical and biomechanical events

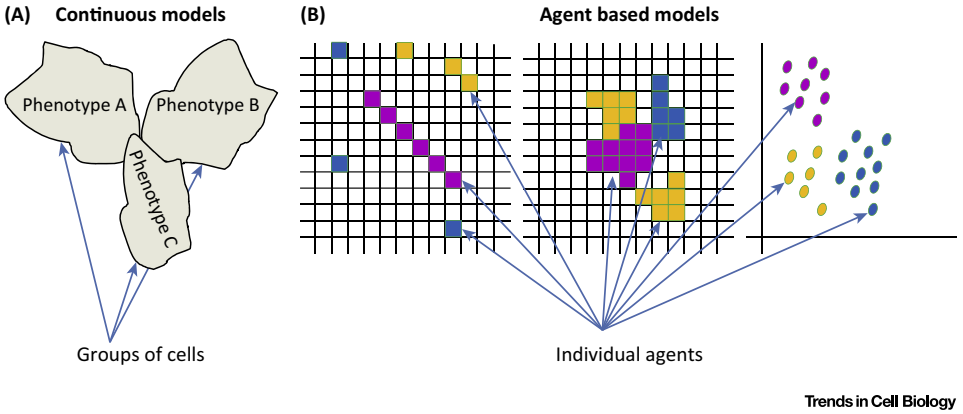

Figure 4. *In Silico* Computational Models for the Study of Cell Migration. (A) Continuous models treat cells as populations sharing specific properties (phenotypes). (B) Agent-based models represent individual agents as entities occupying a single grid square (cellular automaton, left), entities composed of different grid squares defining cell shape and size (cellular Potts model, middle), and entities occupying a grid-free space (nuclei-centered model, right).

components therefore need to be converted into a set of mathematical equations that describe the temporal and spatial evolution of the system. In this case differential equation systems are used, and the resulting models are referred to as continuous (or continuum) models because cells are represented by continuous variables. Conversely, we refer to agent-based (or individual-based) models (ABMs) for models that handle cells as discrete objects. This broad classification is schematically shown in Figure 4. The next two sections of this review summarize continuous models and ABMs for the simulation of cell migration.

Continuous Models

In continuous models cells are represented as populations of objects whose properties are defined as averages for the whole cell population (Figure 4A). This type of modeling is therefore more practical at population scales where modeling each cell as a single entity can be computationally prohibitive. By definition, these models are deterministic, and the number of cell phenotypes must be specified in advance. Continuous models are described with differential equations (Box 3) and have found diverse applications in cancer cell migration studies. A continuous spatial model of tumor–host interaction can be found in [121]; this model takes into account the complex interactions between the tumor and surrounding stromal cells by including densities of endothelial cells and the ECM. Hybrid-modeling frameworks, where the tumor tissue is modeled using both discrete (cell-scale) and continuum (tumor-scale) elements, have also been presented [122]. Finally, the impact of cell adhesion on cellular invasion processes in both cancer and development has been simulated using a continuous model [123].

Agent-Based Models

The concept of an ABM refers to a different philosophy than that used in differential equation systems. In ABMs (Figure 4B), individual agents interact with the environment and other agents according to a set of rules, and make decisions that lead to a particular behavior. ABMs account for probabilistic uncertainty, or stochasticity; for example, an individual agent can change its location at a given probability instead of following a deterministic process. The ability to account for individual diversity is an advantage of ABMs. However, it also implies large computational complexity, and ABMs require hours or even days to run a single simulation. Furthermore, stochastic ABMs need to be simulated numerous times to obtain the overall average behavior of the system. Therefore, these models are often applied when the number of individual interacting units, such as cancer cells, is limited and controlled to remain small. The aggregate of agent

Box 3. Differential Equations for Continuous Modeling of Cell Migration

Numerous mathematical approaches can be used when building continuous models for cell migration studies. Mathematical models based on systems of ordinary differential equations (ODEs) are the most common. The key advantage of ODE modeling is that this model structure has been extensively applied in the study of various physical phenomena, and is therefore well-established. Furthermore, the mathematical analysis of these systems is relatively simple compared to other types of models, and their solutions can be computationally simulated with great efficiency. However, ODEs do not capture spatial dynamics or stochastic effects.

Systems of ODEs are finite-dimensional systems, while delay differential equations (DDEs) and partial differential equations (PDEs) are infinite-dimensional systems. As a result, DDEs and PDEs require more computational and analytical complexity. In general, DDE models are similar in structure to ODE models, except that they explicitly include time-delays. DDEs are simpler than PDEs, and only slightly more complex than ODEs to simulate numerically, which means that, with only a slight increase in computational complexity, DDE models widely expand the repertoire of phenomena that can be modeled. PDEs are able to capture more complexity than DDEs and ODEs, taking into account both spatial dynamics and age-based behavior, that is, describing the progression of cells through a scheduled development process. However, these models tend to be significantly more computationally demanding than ODE and DDE systems. Finally, stochastic differential equations (SDEs) lie between deterministic differential equation models and agent-based models (ABMs). SDEs are similar in formulation to ODEs, except that they allow their variables to take random values.

behaviors over time produces high-level, emergent phenomena, and inclusion of multiple types of agents allows exploration of complex behaviors. For example, a recent study [124,125] developed a cell migration model where both the actomyosin cortex and the outer cell membrane are represented as a set of agents. The model incorporates cell morphology, plasma-membrane blebbing, lamellipodia formation, and interactions with the ECM filaments, and furthermore explores cell migration mode transitions upon changes in matrix environments, a phenomenon otherwise difficult to probe in an experimental setup.

ABMs can be subdivided into nuclei-centered models and deformable cell models, depending on how much cellular structural detail is incorporated. In the nuclei-centered models individual cells are represented in space by their nuclei, while in the deformable cell models cells are single entities characterized by a deformable shape and area (or volume) which can vary in time depending on the cell state (and thus on growth, division, and migration) as well as on the interaction with surrounding cells.

Cellular automata (CA) are the most common ABMs. CA are based on a lattice of points (cells), each capable of a finite number of states, represented by one or more discrete or continuous variables. Each cell is connected to a finite number of neighbor cells, whose states at time t_n result in a new state at time t_{n+1}. A set of rules describes the evolution of the agents' state and their position, where both the state change and the movement of a specific agent depend on the current state of the agent and the states of the surrounding agents [126] (Figure 5). One attractive aspect of CA is their ability to deal with multiple scales at the same time, enabling for instance the analysis of tumor invasion [116], a phenomenon that can be viewed as a property of the tissue scale that emerges from the population of migratory individual cells at lower scales [127].

Two different types of CA are the lattice-gas-based CA (LGCA) and the cellular Potts model (CPM). Similarly to other types of CA, the LGCA employ a lattice and include a finite set of cell states, an interaction across neighboring cells, as well as local rules that define movements and transitions between states. LGCA differ from CA by assuming cell motion, together with an exclusion principle; that is, the connectivity of the lattice fixes the number of allowed velocities for each cell in the grid. LGCA models are efficient for simulating the migratory behavior of cells that retain simple cell shapes during translocation, but are not appropriate for analyzing cells such as amoebae that drastically change their shapes during migration. In this case, CPMs are preferred

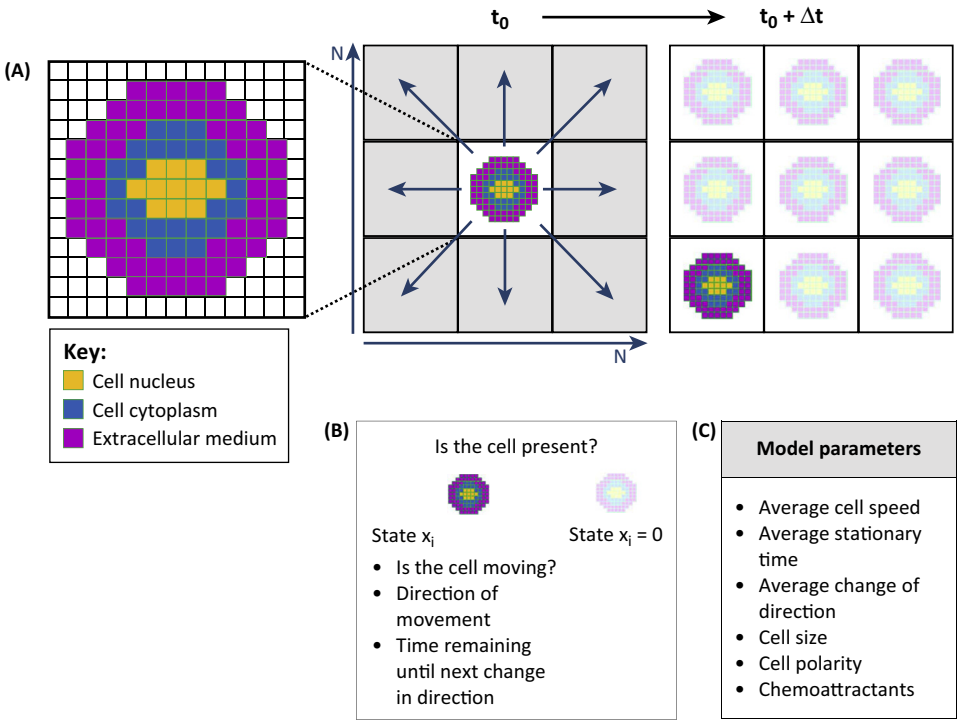

Figure 5. A Schematic Representation of a Two-Level Agent-Based Model Employing a Regular Square Lattice. (A) At the first level, single agents simulate the cell nucleus, cell cytoplasm, and the extracellular medium for single cells, while at the second level agents represent single cells. Each computational site, surrounded by eight nearest neighbors, can either be occupied by a single cell, or be free and therefore available for cell movement. At equally spaced timepoints (with time-interval Δt), the state x_i of each automaton i (i = 1, 2, . . ., NxN, where N is the dimension of the grid) evolves through interaction with the neighboring sites. (B) The agent state x_i is defined according to a set of rules, and (C) model parameters are estimated from experimental data.

[126,128]. CPMs have been successfully used for the numerical simulation of tumor invasion [129], of cell migration on and in the ECM [130], and to elucidate the role of the ECM in glioma invasion [131]. Recently, a CPM has been integrated into a multiscale framework for the simulation of cell migration during morphogenesis [132]. Immunological studies have also benefited from CPMs [133], as has the characterization of neuronal migration in the developing cortex [134].

A rich set of publications has recently presented the effects of the **tumor microenvironment** in tumor cell invasion through numerical simulations [117,127]. Some of these models are hybrid, in other words they combine a continuum deterministic model of variables and a discrete CA-like model of individual tumor cell migration. In the evolutionary hybrid CA, the variable accounting for the tumor microenvironment is the concentration of oxygen. The immersed boundary cell (IBCell) model is instead able to capture the morphology of fully deformable cells, especially during their individual or collective migration. Here, the variables that account for the tumor microenvironment are mechanical forces emanating from cell–cell and cell–ECM interactions. Finally, in the hybrid discrete-continuum model, the tumor microenvironment is reduced to oxygen, proteases, and ECM. Recently, a generalized CA model has been developed that takes into account a set of microscopic scale tumor–host interactions, including mechanical interactions between tumor cells and stroma, the degradation of the ECM by invasive cells, and oxygen gradient-driven cell motion [135].

Other models are also available for numerical simulations of cell migration. For example, probabilistic finite element models have been developed for single-cell migration in 3D [136], and simple stochastic models have been used for the study of collective cell migration in epithelial sheets [137].

Software Tools for Cell Migration *In Silico* Modeling

Mathematical models need to be implemented computationally. A common approach is to write the relevant, specific computational software for each problem. However, various software packages are also available for most of the modeling paradigms. Several tools handle the numerical solution of differential equation systems, such as the freely-available Process Modeling Tool (Promot) [138] and the commercial Simulation Control Program (Scop) [139]. Generic modeling packages such as Mathematica or MATLAB are also used, although these tools are not customized to support biological simulation *per se*. More specialized solutions are also available, for example, the Virtual Cell [140,141], a unique computational framework for the modeling and simulation of cell biology. This system allows biologists with little training in physics and mathematics to engage in computational cell biology: a graphical user interface guides the construction of cell models by specifying the molecules, reactions, and structures involved. These biological models are then converted into differential equation systems, and numerical simulations are produced by the software based on these equations. Most Virtual Cell models that have been developed for the simulation of cell migration and invasion phenomena are stored in a database which is equipped with links to external databases, such as Swiss-Prot [142] or KEGG [143], to facilitate integration with other existing resources. Furthermore, a set of tools is available that make use of systems biology markup language (SBML), a representation format based on XML that is widely used for storing and sharing biological models.

In addition to the Virtual Cell, other simulation environments for multi- or single-cell-based modeling include the CompuCell3D [144], based on CPMs, and the hybrid solution Cell++ [145], together with other software packages and simulation tools developed by the CellML [146] project. Furthermore, a large number of specific SBML tools have been recently developed, including the SBML ODE Solver [147], MathSBML [148], the SBML ToolBox [149], and the SBW–MATLAB interface [150]. The Systems Biology Workshop [151] also provides an infrastructure platform and computing environment for biological modeling and simulation, and brings together various software components such as model editors, simulators, and data analyzer/visualizers.

Concluding Remarks

Cell migration is a complex, multiscale process, occurring in both physiological and pathological phenomena, and as such is worthy of in-depth investigation and analysis. Advances in automated image acquisition and image processing have, however, created a pressing need in the field for the development of new computational methods and tools for the quantification of cell migration experiments. Furthermore, the recent integration of *in vitro* setups with *in silico* numerical simulations has been shown to be a promising tool for a systems-biology understanding of this process. Despite the myriad of algorithms, tools, and even models addressed in this review, several key questions remain to be answered (see Outstanding Questions). Indeed, although cell migration research is increasingly morphing into a *de facto* high-content and high-throughput discipline, the field is not yet able to maximally exploit the rich datasets being produced because of the following reasons: (i) image-processing algorithms are often developed to work for specific experimental conditions; (ii) poor attention is paid to data annotation, management, and sharing; and (iii) the integration of *in vitro* experiments with *in silico* models is not yet fully exploited.

To address these challenges, important developments are needed. First, imaging benchmark datasets are desired to enable the evaluation of algorithms on a variety of cell lines and imaging

Outstanding Questions

In 1980, Abercrombie concluded his Croonian lecture with the following words: 'It seems to me that comprehensiveness is wanted in the subject [of migration], which is still inclined to suffer from fragmentation.' A fragmentation that, 35 years later, still persists. What can we do to overcome this fragmentation?

As a result of the complexity of cell migration, with its multi-scale and multi-parametric nature, many conflicting results have been produced from cell migration experiments over the years. Are we observing truly different migratory behavior, or could it be that these data all describe the same overall behavior under different conditions?

Can we build a single, integrated mathematical model to help us to understand the quantitative and qualitative origins of this observed heterogeneity of cell migration behaviors?

To be truly useful, mathematical models need to be predictive and quantitative, rather than a qualitative afterthought. How can we stimulate the interaction between experimentalists and modelers in the field in order that development and validation of the models can occur in a cyclic experimental context?

While dozens of algorithms have been developed to address cell segmentation and tracking tasks, their relative and absolute performance mostly remains unclear, especially across different experimental setups. How can we procure reliable and realistic benchmark datasets where the ground truth is truly known? In addition, how can we stimulate the benchmarking of proposed new tools in a transparent way, with results accessible to the entire community?

Other high-throughput fields in the life sciences have already shown that data annotation, standardization, and sharing can lead to exciting new discoveries. How can we bring this paradigm to the field of cell migration? Which new tools will allow us to perform such integrative data mining?

conditions. The results of the assessment of new algorithms on these benchmarks also need to be published such that prospective users can tailor their choice to the most powerful algorithm or tool. Second, the field needs to direct more attention towards data annotation, management, and sharing, which will in turn enable quality control, data exchange, and meta-analyses [24]. Unfortunately, few bioinformatics tools have been developed to meet these needs. The CellProfiler Analyst module of the CellProfiler software [100] implements a plate viewer object through which the user can define essential metadata, such as the plate format used in the experiment. Analyzed data are then stored in a local database and can be retrieved later for further interpretation. The CellMissy software [152] enables annotation of both technical and biological conditions, stores quantitative data and experimental settings in a relational database, and provides options for data export and sharing with other CellMissy users. Further development and use of software tools for the annotation and management of cell migration experiments will certainly be crucial. Additionally, data-exchange options will create future possibilities for integration and comparison across different datasets and across research laboratories [24], which has already been seen for other scientific domains such as proteomics and genomics. A first endeavor in the direction of cell migration data-sharing has been carried out in the first World Cell Race [153], where 54 different cell types from various animals and tissues were provided by 47 laboratories. This collaboration has enabled, for the first time, a large-scale analysis of cell migration data, in turn allowing researchers to elaborate a new model describing an actin flow-mediated coupling between cell speed and cell persistence [154]. This constitutes a clear example of how scientific games or competitions involving large-scale experiments can lead to the identification and understanding of novel and relevant biological processes which might otherwise escape observation. Finally, further combinations of wet-lab data and computational modeling will enable new research hypotheses to be generated and validated, unlocking both novel fundamental knowledge and innovative translations of this knowledge into the (pre)clinical world.

Acknowledgments

The authors acknowledge funding from the European Commission Horizon 2020 Programme under Grant Agreement 634107 (PHC32-2014) 'MULTIMOT'. P.M. and M.V.T. acknowledge funding from the Faculty of Medicine and Health Sciences, Ghent University, Ghent, Belgium.

Resources

[1] www.dcilabs.com/productsheets/productsheet_MIA.pdf
[2] www.thermoscientific.com/en/products/cellular-imaging-analysis.html
[3] www.mediacy.com/index.aspx?page=IPP
[4] www.bitplane.com/imaris/imaristrack
[5] www.moleculardevices.com
[6] www.perkinelmer.com/pages/020/cellularimaging/products/openlab.xhtml
[7] https://bitbucket.org/djpbarry/adapt
[8] http://umr168.curie.fr/en/avemap
[9] http://cse-lab.ethz.ch/software/
[10] www.cellcognition.org
[11] www.cellprofiler.org/
[12] http://bio.cse.ohio-state.edu/CellTrack/
[13] http://dbkgroup.org/celltracker/about.php; www2.warwick.ac.uk/fac/sci/systemsbiology/staff/bretschneider/celltracker
[14] https://sites.google.com/site/itrack4usoftware/home
[15] www2.warwick.ac.uk/fac/sci/systemsbiology/staff/bretschneider/lineagetracker
[16] http://icy.bioimageanalysis.org/plugin/Manual_Tracking
[17] www.imagescience.org/meijering/software/mtrackj/
[18] www.cs.tau.ac.il/~assafzar/
[19] https://universityofcolorado.app.box.com/s/qzs6nos4470sjfsaw8wg
[20] http://icy.bioimageanalysis.org/plugin/Spot_Tracking
[21] http://cse-lab.ethz.ch/software/

[22] http://fiji.sc/TrackMate

[23] http://lccb.hms.harvard.edu/software.html

[24] www.perkinelmer.com/pages/020/cellularimaging/products/volocity.xhtml

References

1. Aman, A. and Piotrowski, T. (2010) Cell migration during morphogenesis. *Dev. Biol.* 341, 20–33
2. Vicente-Manzanares, M. and Horwitz, A.R. (2011) Cell migration: an overview. *Methods Mol. Biol.* 769, 1–24
3. Theveneau, E. and Mayor, R. (2012) Neural crest delamination and migration: from epithelium-to-mesenchyme transition to collective cell migration. *Dev. Biol.* 366, 34–54
4. Friedl, P. *et al.* (2012) Classifying collective cancer cell invasion. *Nat. Cell Biol.* 14, 777–783
5. Li, L. *et al.* (2013) Collective cell migration: implications for wound healing and cancer invasion. *Burns Trauma* 1, 21
6. Cooper, J.A. (2013) Cell biology in neuroscience: mechanisms of cell migration in the nervous system. *J. Cell Biol.* 202, 725–734
7. Teijeira, A. *et al.* (2014) Taking the lymphatic route: dendritic cell migration to draining lymph nodes. *Semin. Immunopathol.* 36, 261–274
8. Reig, G. *et al.* (2014) Cell migration: from tissue culture to embryos. *Development* 141, 1999–2013
9. Sanz-Moreno, V. and Marshall, C.J. (2010) The plasticity of cytoskeletal dynamics underlying neoplastic cell migration. *Curr. Opin. Cell Biol.* 22, 690–696
10. Wells, A. *et al.* (2013) Targeting tumor cell motility as a strategy against invasion and metastasis. *Trends Pharmacol. Sci.* 34, 283–289
11. Biro, M. *et al.* (2014) Targeting Rho-GTPases in immune cell migration and inflammation. *Br. J. Pharmacol.* 171, 5491–5506
12. Cockle, J.V. *et al.* (2015) Cell migration in paediatric glioma; characterisation and potential therapeutic targeting. *Br. J. Cancer* 112, 693–703
13. Ashby, W.J. and Zijlstra, A. (2012) Established and novel methods of interrogating two-dimensional cell migration. *Integr. Biol.* 4, 1338–1350
14. Kramer, N. *et al.* (2013) In vitro cell migration and invasion assays. *Mutat. Res.* 752, 10–24
15. Friedl, P. *et al.* (2012) New dimensions in cell migration. *Nat. Rev. Mol. Cell Biol.* 13, 743–747
16. Doyle, A.D. *et al.* (2013) Dimensions in cell migration. *Curr. Opin. Cell Biol.* 25, 642–649
17. Yarrow, J.C. *et al.* (2005) Screening for cell migration inhibitors via automated microscopy reveals a Rho-kinase inhibitor. *Chem. Biol.* 12, 385–395
18. Hulkower, K.I. and Herber, R.L. (2011) Cell migration and invasion assays as tools for drug discovery. *Pharmaceutics* 3, 107–124
19. Zhou, Z.N. *et al.* (2011) Tumor-stroma: In vivo assays and intravital imaging to study cell migration and metastasis. *Drug Discov. Today Dis. Models* 8, 95–112
20. Leong, H.S. *et al.* (2012) Assessing cancer cell migration and metastatic growth in vivo in the chick embryo using fluorescence intravital imaging. *Methods Mol. Biol.* 872, 1–14
21. Patsialou, A. *et al.* (2013) Intravital multiphoton imaging reveals multicellular streaming as a crucial component of in vivo cell migration in human breast tumors. *Intravital* 2, e25294
22. Benechet, A.P. *et al.* (2014) Visualizing T cell migration in situ. *Front. Immunol.* 5, 363
23. Munoz, M.A. *et al.* (2014) T cell migration in intact lymph nodes in vivo. *Curr. Opin. Cell Biol.* 30, 17–24
24. Masuzzo, P. and Martens, L. (2015) An open data ecosystem for cell migration research. *Trends Cell Biol.* 25, 55–58
25. Danuser, G. *et al.* (2013) Mathematical modeling of eukaryotic cell migration: insights beyond experiments. *Annu. Rev. Cell Dev. Biol.* 29, 501–528
26. Kam, Y. *et al.* (2012) Cellular modeling of cancer invasion: integration of in silico and in vitro approaches. *J. Cell. Physiol.* 227, 431–438
27. Debeir, O. *et al.* (2008) Models of cancer cell migration and cellular imaging and analysis. In *The Motile Actin System in Health and Disease* (Lambrechts, A. and Ampe, C., eds), pp. 123–156, Transworld Research Network
28. Eils, R. and Athale, C. (2003) Computational imaging in cell biology. *J. Cell Biol.* 161, 477–481
29. Dormann, D. and Weijer, C.J. (2006) Imaging of cell migration. *EMBO J.* 25, 3480–3493
30. Combs, C.A. (2001) Fluorescence microscopy: a concise guide to current imaging methods. *Curr. Protoc. Neurosci.* 50, 2.1.1–2.1.14
31. Boutet de Monvel, J. *et al.* (2001) Image restoration for confocal microscopy: improving the limits of deconvolution, with application to the visualization of the mammalian hearing organ. *Biophys. J.* 80, 2455–2470
32. Gerlich, D. *et al.* (2003) Quantitative motion analysis and visualization of cellular structures. *Methods* 29, 3–13
33. Biggs, D.S.C. (2010) A practical guide to deconvolution of fluorescence microscope imagery. *Microsc. Today* 18, 10
34. Sekko, E. *et al.* (1999) A deconvolution technique using optimal Wiener filtering and regularization. *Signal Process.* 72, 23–32
35. Ramani, S. *et al.* (2008) Deconvolution of 3D fluorescence micrographs with automatic risk minimization. In *5th IEEE International Symposium on Biomedical Imaging: From Nano to Macro*, pp. 732–735, IEEE
36. Sarder, P. and Nehorai, A. (2006) Deconvolution methods for 3-D fluorescence microscopy images. *IEEE Signal Process. Mag.* 23, 32–45
37. Soulez, F. *et al.* (2012) Blind deconvolution of 3D data in wide field fluorescence microscopy. In *9th IEEE International Symposium on Biomedical Imaging (ISBI)*, pp. 1735–1738, IEEE
38. Agard, D.A. (1984) Optical sectioning microscopy: cellular architecture in three dimensions. *Annu. Rev. Biophys. Bioeng.* 13, 191–219
39. Keuper, M. *et al.* (2012) Blind deconvolution with PSF regularization for wide-field microscopy. In *9th IEEE International Symposium on Biomedical Imaging (ISBI)*, pp. 1292–1295, IEEE
40. Vonesch, C. and Unser, M. (2009) A fast multilevel algorithm for wavelet-regularized image restoration. *IEEE Trans. Image Process.* 18, 509–523
41. Dupe, F-X. *et al.* (2008) Deconvolution of confocal microscopy images using proximal iteration and sparse representations. In *5th IEEE International Symposium on Biomedical Imaging: From Nano to Macro*, pp. 736–739, IEEE
42. Ben Hadj, S. and Blanc-Feraud, L. (2012) Modeling and removing depth variant blur in 3D fluorescence microscopy. In *IEEE International Conference on Acoustics, Speech and Signal Processing (ICASSP)*, pp. 689–692, IEEE
43. Trepat, X. *et al.* (2012) Cell migration. *Compr. Physiol.* 2, 2369–2392
44. Ilina, O. and Friedl, P. (2009) Mechanisms of collective cell migration at a glance. *J. Cell Sci.* 122, 3203–3208
45. Theveneau, E. and Mayor, R. (2013) Collective cell migration of epithelial and mesenchymal cells. *Cell. Mol. Life Sci.* 70, 3481–3492
46. Huth, J. *et al.* (2010) Significantly improved precision of cell migration analysis in time-lapse video microscopy through use of a fully automated tracking system. *BMC Cell Biol.* 11, 24
47. Zaritsky, A. *et al.* (2013) Benchmark for multi-cellular segmentation of bright field microscopy images. *BMC Bioinformatics* 14, 319
48. Maška, M. *et al.* (2014) A benchmark for comparison of cell tracking algorithms. *Bioinformatics* 30, 1609–1617
49. Wu, Q. *et al.* (2010) *Microscope Image Processing,* Academic Press

50. Sankur, B. (2004) Survey over image thresholding techniques and quantitative performance evaluation. *J. Electron. Imaging* 13, 146
51. Gonzalez, R.C. and Woods, R.E. (2008) *Digital Image Processing*. (3rd edn), Prentice Hall
52. Wählby, C. *et al.* (2004) Combining intensity, edge and shape information for 2D and 3D segmentation of cell nuclei in tissue sections. *J. Microsc.* 215, 67–76
53. Yang, X. *et al.* (2006) Nuclei segmentation using marker-controlled watershed, tracking using mean-shift, and Kalman Filter in time-lapse microscopy. *IEEE Trans. Circ. Syst. I: Regul. Papers* 53, 2405–2414
54. Lin, G. *et al.* (2007) A multi-model approach to simultaneous segmentation and classification of heterogeneous populations of cell nuclei in 3D confocal microscope images. *Cytometry A* 71, 724–736
55. Ali, R. *et al.* (2008) Advanced phase-based segmentation of multiple cells from brightfield microscopy images. In *5th IEEE International Symposium on Biomedical Imaging: From Nano to Macro*, pp. 181–184, IEEE
56. Zordan, M.D. *et al.* (2011) A high throughput, interactive imaging, bright-field wound healing assay. *Cytometry A* 79, 227–232
57. Yin, Z. *et al.* (2010) Cell segmentation in microscopy imagery using a bag of local Bayesian classifiers. In *2010 IEEE International Symposium on Biomedical Imaging: From Nano to Macro*, pp. 125–128, IEEE
58. Zaritsky, A. *et al.* (2011) Cell motility dynamics: a novel segmentation algorithm to quantify multi-cellular bright field microscopy images. *PLoS ONE* 6, e27593
59. Gebäck, T. *et al.* (2009) TScratch: a novel and simple software tool for automated analysis of monolayer wound healing assays. *Biotechniques* 46, 265–274
60. Topman, G. *et al.* (2012) A standardized objective method for continuously measuring the kinematics of cultures covering a mechanically damaged site. *Med. Eng. Phys.* 34, 225–232
61. Kass, A. *et al.* (1988) Snakes: active contour models. *Int. J. Comput. Vis.* 1988, 321–333
62. Cohen, L.D. (1991) On active contour models and balloons. *CVGIP: Image Underst.* 53, 211–218
63. Ray, N. and Acton, S.T. (2002) Active contours for cell tracking. In *Proceedings Fifth IEEE Southwest Symposium on Image Analysis and Interpretation*, pp. 274–278, IEEE
64. Li, K. *et al.* (2008) Cell population tracking and lineage construction with spatiotemporal context. *Med. Image Anal.* 12, 546–566
65. Yang, F. *et al.* (2005) Cell segmentation, tracking, and mitosis detection using temporal context. *Med. Image Comput. Comput. Assist. Interv.* 8, 302–309
66. Dufour, A. *et al.* (2005) Segmenting and tracking fluorescent cells in dynamic 3-D microscopy with coupled active surfaces. *IEEE Trans. Image Process.* 14, 1396–1410
67. Dzyubachyk, O. *et al.* (2010) Advanced level-set-based cell tracking in time-lapse fluorescence microscopy. *IEEE Trans. Med. Imaging* 29, 852–867
68. Cheng, Y. (1995) Mean shift, mode seeking, and clustering. *IEEE Trans. Pattern Anal. Mach. Intell.* 17, 790–799
69. Liu, J.S. (2008) *Monte Carlo Strategies in Scientific Computing*, Springer Science & Business Media
70. Smal, I. *et al.* (2008) Particle filtering for multiple object tracking in dynamic fluorescence microscopy images: application to microtubule growth analysis. *IEEE Trans. Med. Imaging* 27, 789–804
71. Rapoport, D.H. *et al.* (2011) A novel validation algorithm allows for automated cell tracking and the extraction of biologically meaningful parameters. *PLoS ONE* 6, e27315
72. Kanade, T. *et al.* (2011) Cell image analysis: Algorithms, system and applications. In *IEEE Workshop on Applications of Computer Vision (WACV)*, pp. 374–381, IEEE
73. Huh, S. *et al.* (2011) Automated mitosis detection of stem cell populations in phase-contrast microscopy images. *IEEE Trans. Med. Imaging* 30, 586–596
74. Amat, F. and Keller, P.J. (2013) 3D Haar-like elliptical features for object classification in microscopy. In *IEEE 10th International Symposium on Biomedical Imaging*, pp. 1194–1197, IEEE
75. Friedl, P. and Gilmour, D. (2009) Collective cell migration in morphogenesis, regeneration and cancer. *Nat. Rev. Mol. Cell Biol.* 10, 445–457
76. Rørth, P. (2009) Collective cell migration. *Annu. Rev. Cell Dev. Biol.* 25, 407–429
77. Rørth, P. (2012) Fellow travellers: emergent properties of collective cell migration. *EMBO Rep.* 13, 984–991
78. Riahi, R. *et al.* (2012) Advances in wound-healing assays for probing collective cell migration. *J. Lab. Autom.* 17, 59–65
79. Anon, E. *et al.* (2012) Cell crawling mediates collective cell migration to close undamaged epithelial gaps. *Proc. Natl. Acad. Sci. U.S.A.* 109, 10891–10896
80. Meyvantsson, I. and Beebe, D.J. (2008) Cell culture models in microfluidic systems. *Annu. Rev. Anal. Chem.* 1, 423–449
81. Liang, C-C. *et al.* (2007) In vitro scratch assay: a convenient and inexpensive method for analysis of cell migration in vitro. *Nat. Protoc.* 2, 329–333
82. Ranzato, E. *et al.* (2011) Wound healing properties of jojoba liquid wax: an in vitro study. *J. Ethnopharmacol.* 134, 443–449
83. Walter, M.N.M. *et al.* (2010) Mesenchymal stem cell-conditioned medium accelerates skin wound healing: an in vitro study of fibroblast and keratinocyte scratch assays. *Exp. Cell Res.* 316, 1271–1281
84. Büth, H. *et al.* (2007) Cathepsin B is essential for regeneration of scratch-wounded normal human epidermal keratinocytes. *Eur. J. Cell Biol.* 86, 747–761
85. Simpson, K.J. *et al.* (2008) Identification of genes that regulate epithelial cell migration using an siRNA screening approach. *Nat. Cell Biol.* 10, 1027–1038
86. Supatto, W. *et al.* (2005) In vivo modulation of morphogenetic movements in Drosophila embryos with femtosecond laser pulses. *Proc. Natl. Acad. Sci. U.S.A.* 102, 1047–1052
87. Raffel, M. *et al.* (2007) *Particle Image Velocimetry: A Practical Guide*, Springer Science & Business Media
88. Petitjean, L. *et al.* (2010) Velocity fields in a collectively migrating epithelium. *Biophys. J.* 98, 1790–1800
89. Milde, F. *et al.* (2012) Cell Image Velocimetry (CIV): boosting the automated quantification of cell migration in wound healing assays. *Integr. Biol.* 4, 1437–1447
90. Friedl, P. and Wolf, K. (2010) Plasticity of cell migration: a multiscale tuning model. *J. Exp. Med.* 207, 11–19
91. Huttenlocher, A. and Horwitz, A.R. (2011) Integrins in cell migration. *Cold Spring Harb. Perspect. Biol.* 3, a005074
92. Maheshwari, G. and Lauffenburger, D.A. (1998) Deconstructing (and reconstructing) cell migration. *Microsc. Res. Tech.* 43, 358–368
93. Mokhtari, Z. *et al.* (2013) Automated characterization and parameter-free classification of cell tracks based on local migration behavior. *PLoS ONE* 8, e80808
94. Gorelik, R. and Gautreau, A. (2014) Quantitative and unbiased analysis of directional persistence in cell migration. *Nat. Protoc.* 9, 1931–1943
95. Beltman, J.B. *et al.* (2009) Analysing immune cell migration. *Nat. Rev. Immunol.* 9, 789–798
96. Pincus, Z. and Theriot, J.A. (2007) Comparison of quantitative methods for cell-shape analysis. *J. Microsc.* 227, 140–156
97. Murray, J.I. *et al.* (2006) The lineaging of fluorescently-labeled Caenorhabditis elegans embryos with StarryNite and AceTree. *Nat. Protoc.* 1, 1468–1476
98. Abràmoff, M.D. *et al.* (2004) Image processing with Image. *J. Biophotonics Int.* 11, 36–42
99. Schindelin, J. *et al.* (2012) Fiji: an open-source platform for biological-image analysis. *Nat. Methods* 9, 676–682
100. Carpenter, A.E. *et al.* (2006) CellProfiler: image analysis software for identifying and quantifying cell phenotypes. *Genome Biol.* 7, R100
101. De Chaumont, F. *et al.* (2012) Icy: an open bioimage informatics platform for extended reproducible research. *Nat. Methods* 9, 690–696
102. Deforet, M. *et al.* (2012) Automated velocity mapping of migrating cell populations (AVeMap). *Nat. Methods* 9, 1081–1083

103. Taylor, Z.J. *et al.* (2010) Long-duration time-resolved PIV to study unsteady aerodynamics. *IEEE Trans. Instrum. Meas.* 59, 3262–3269

104. Chapnick, D.A. *et al.* (2013) The development of a novel high throughput computational tool for studying individual and collective cellular migration. *PLoS ONE* 8, e82444

105. Culjak, I. *et al.* (2013) A brief introduction to OpenCV. In *Proceedings of the 35th International MIPRO Convention*, pp. 2142–2147, IEEE

106. Sacan, A. *et al.* (2008) CellTrack: an open-source software for cell tracking and motility analysis. *Bioinformatics* 24, 1647–1649

107. Van der Walt, S. *et al.* (2014) scikit-image: image processing in Python. *PeerJ* 2, e453

108. Goldberg, I.G. *et al.* (2005) The open microscopy environment (OME) data model and XML file: open tools for informatics and quantitative analysis in biological imaging. *Genome Biol.* 6, R47

109. Held, M. *et al.* (2010) CellCognition: time-resolved phenotype annotation in high-throughput live cell imaging. *Nat. Methods* 7, 747–754

110. Sommer, C. *et al.* (2013) CellH5: a format for data exchange in high-content screening. *Bioinformatics* 29, 1580–1582

111. Lock, J.G. and Strömblad, S. (2010) Systems microscopy: an emerging strategy for the life sciences. *Exp. Cell Res.* 316, 1438–1444

112. Le Dévédec, S.E. *et al.* (2010) Systems microscopy approaches to understand cancer cell migration and metastasis. *Cell. Mol. Life Sci.* 67, 3219–3240

113. Eddy, J.A. *et al.* (2015) Fostering synergy between cell biology and systems biology. *Trends Cell Biol.* 25, 440–445

114. Rosello, C. *et al.* (2004) Model driven quantification of individual and collective cell migration. *Acta Biotheor.* 52, 343–363

115. Safferling, K. *et al.* (2013) Wound healing revised: a novel reepithelialization mechanism revealed by in vitro and in silico models. *J. Cell Biol.* 203, 691–709

116. Sanga, S. *et al.* (2007) Predictive oncology: a review of multidisciplinary, multiscale in silico modeling linking phenotype, morphology and growth. *Neuroimage* 37 (Suppl. 1), S120–S134

117. Anderson, A.R.A. and Quaranta, V. (2008) Integrative mathematical oncology. *Nat. Rev. Cancer* 8, 227–234

118. Lock, J.G. *et al.* (2014) Plasticity in the macromolecular-scale causal networks of cell migration. *PLoS ONE* 9, e90593

119. Bergert, M. *et al.* (2015) Force transmission during adhesion-independent migration. *Nat. Cell Biol.* 17, 524–529

120. Liu, Y-J. *et al.* (2015) Confinement and low adhesion induce fast amoeboid migration of slow mesenchymal cells. *Cell* 160, 659–672

121. Hinow, P. *et al.* (2009) A spatial model of tumor-host interaction: application of chemotherapy. *Math. Biosci. Eng.* 6, 521–546

122. Lowengrub, J.S. *et al.* (2010) Nonlinear modelling of cancer: bridging the gap between cells and tumours. *Nonlinearity* 23, R1–R91

123. Painter, K.J. *et al.* (2010) The impact of adhesion on cellular invasion processes in cancer and development. *J. Theor. Biol.* 264, 1057–1067

124. Tozluoğlu, M. *et al.* (2013) Matrix geometry determines optimal cancer cell migration strategy and modulates response to interventions. *Nat. Cell Biol.* 15, 751–762

125. Tozluoglu, M. *et al.* (2015) Cost–benefit analysis of the mechanisms that enable migrating cells to sustain motility upon changes in matrix environments. *J. R. Soc. Interface* 12, 20141355

126. Alber, M.S. *et al.* (2003) On cellular automaton approaches to modeling biological cells. In *Mathematical Systems Theory in Biology, Communication, and Finance* (Rosenthal, J. and Gilliam, D.S., eds), pp. 1–39, Springer

127. Quaranta, V. *et al.* (2008) Invasion emerges from cancer cell adaptation to competitive microenvironments: quantitative predictions from multiscale mathematical models. *Semin. Cancer Biol.* 18, 338–348

128. Anderson, A.R.A. *et al.*, eds (2007) *Single-Cell-Based Models in Biology and Medicine*, Birkhäuser Basel

129. Szabó, A. and Merks, R.M.H. (2013) Cellular Potts modeling of tumor growth, tumor invasion, and tumor evolution. *Front. Oncol.* 3, 87

130. Scianna, M. *et al.* (2013) A cellular Potts model simulating cell migration on and in matrix environments. *Math. Biosci. Eng.* 10, 235–261

131. Rubenstein, B.M. and Kaufman, L.J. (2008) The role of extracellular matrix in glioma invasion: a cellular Potts model approach. *Biophys. J.* 95, 5661–5680

132. Voss-Böhme, A. (2012) Multi-scale modeling in morphogenesis: a critical analysis of the cellular Potts model. *PLoS ONE* 7, e42852

133. Vroomans, R.M.A. *et al.* (2012) Chemotactic migration of T cells towards dendritic cells promotes the detection of rare antigens. *PLoS Comput. Biol.* 8, e1002763

134. Setty, Y. *et al.* (2011) How neurons migrate: a dynamic in-silico model of neuronal migration in the developing cortex. *BMC Syst. Biol.* 5, 154

135. Jiao, Y. and Torquato, S. (2011) Emergent behaviors from a cellular automaton model for invasive tumor growth in heterogeneous microenvironments. *PLoS Comput. Biol.* 7, e1002314

136. Borau, C. *et al.* (2014) Probabilistic Voxel-FE model for single cell motility in 3D. *In Silico Cell Tissue Sci.* 1, 2

137. Sepúlveda, N. *et al.* (2013) Collective cell motion in an epithelial sheet can be quantitatively described by a stochastic interacting particle model. *PLoS Comput. Biol.* 9, e1002944

138. Mirschel, S. *et al.* (2009) ProMoT: modular modeling for systems biology. *Bioinformatics* 25, 687–689

139. Kootsey, J.M. *et al.* (1986) SCoP: an interactive simulation control program for micro- and minicomputers. *Bull. Math. Biol.* 48, 427–441

140. Slepchenko, B.M. *et al.* (2003) Quantitative cell biology with the virtual cell. *Trends Cell Biol.* 13, 570–576

141. Moraru, I.I. *et al.* (2008) Virtual Cell modelling and simulation software environment. *IET Syst. Biol.* 2, 352–362

142. Bairoch, A. (1996) The SWISS-PROT protein sequence data bank and its new supplement TREMBL. *Nucleic Acids Res.* 24, 21–25

143. Kanehisa, M. (2000) KEGG: Kyoto Encyclopedia of Genes and Genomes. *Nucleic Acids Res.* 28, 27–30

144. Swat, M.H. *et al.* (2012) Multi-scale modeling of tissues using CompuCell3D. *Methods Cell Biol.* 110, 325–366

145. Sanford, C. *et al.* (2006) Cell++ – simulating biochemical pathways. *Bioinformatics* 22, 2918–2925

146. Miller, A.K. *et al.* (2010) An overview of the CellML API and its implementation. *BMC Bioinformatics* 11, 178

147. Machné, R. *et al.* (2006) The SBML ODE Solver Library: a native API for symbolic and fast numerical analysis of reaction networks. *Bioinformatics* 22, 1406–1407

148. Shapiro, B.E. *et al.* (2004) MathSBML: a package for manipulating SBML-based biological models. *Bioinformatics* 20, 2829–2831

149. Keating, S.M. *et al.* (2006) SBMLToolbox: an SBML toolbox for MATLAB users. *Bioinformatics* 22, 1275–1277

150. Wellock, C. *et al.* (2005) The SBW–MATLAB interface. *Bioinformatics* 21, 823–824

151. Gillespie, C.S. *et al.* (2006) Tools for the SBML Community. *Bioinformatics* 22, 628–629

152. Masuzzo, P. *et al.* (2013) CellMissy: a tool for management, storage and analysis of cell migration data produced in wound healing-like assays. *Bioinformatics* 29, 2661–2663

153. Maiuri, P. *et al.* (2012) The first World Cell Race. *Curr. Biol.* 22, R673–R675

154. Maiuri, P. *et al.* (2015) Actin flows mediate a universal coupling between cell speed and cell persistence. *Cell* 161, 374–386

155. Hossain, M.J. *et al.* (2011) An active particle-based tracking framework for 2D and 3D time-lapse microscopy images. *Conf. Proc. IEEE Eng. Med. Biol. Soc.* 2011, 6613–6618

156. Tokunaga, T. *et al.* (2014) Automated detection and tracking of many cells by using 4D live-cell imaging data. *Bioinformatics* 30, i43–i51

157. Schiegg, M. *et al.* (2015) Graphical model for joint segmentation and tracking of multiple dividing cells. *Bioinformatics* 31, 948–956

158. Adanja, I. *et al.* (2011) A new method to address unmet needs for extracting individual cell migration features from a large number of cells embedded in 3D volumes. *PLoS ONE* 6, e22263

159. Pimentel, J.A. *et al.* (2012) A segmentation algorithm for automated tracking of fast swimming unlabelled cells in three dimensions. *J. Microsc.* 245, 72–81

160. Barry, D.J. *et al.* (2015) Open source software for quantification of cell migration, protrusions, and fluorescence intensities. *J. Cell Biol.* 209, 163–180

161. Shen, H. *et al.* (2006) Automatic tracking of biological cells and compartments using particle filters and active contours. *Chemometr. Intell. Lab. Syst.* 82, 276–282

162. Cordelières, F.P. *et al.* (2013) Automated cell tracking and analysis in phase-contrast videos (iTrack4U): development of Java software based on combined mean-shift processes. *PLoS ONE* 8, e81266

163. Downey, M.J. *et al.* (2011) Extracting fluorescent reporter time courses of cell lineages from high-throughput microscopy at low temporal resolution. *PLoS ONE* 6, e27886

164. Meijering, E. *et al.* (2012) Methods for cell and particle tracking. *Methods Enzymol.* 504, 183–200

165. Chenouard, N. *et al.* (2013) Multiple hypothesis tracking for cluttered biological image sequences. *IEEE Trans. Pattern Anal. Mach. Intell.* 35, 2736–3750

166. Jaqaman, K. *et al.* (2008) Robust single-particle tracking in live-cell time-lapse sequences. *Nat. Methods* 5, 695–702